

Renewable based thermal systems for microgrids

Mariana Almeida Garcia da Silva
mariana.garcia.silva@tecnico.ulisboa.pt

Instituto Superior Técnico, Universidade de Lisboa, Portugal
December 2021

Abstract— Buildings have a significant contribution to the total energy consumption in the world, playing, therefore, an important role in reaching a more decarbonized and efficient energy sector. Space heating and cooling represent a large portion of the energy consumption in buildings, making the development and improvement of energy systems for these activities crucial. A system for space heating/cooling using solar energy and atmospheric air as heat sources was modeled in Simulink. The main elements of the system were a solar collector, a hot water tank, a storage tank, fan coils, and an air-water heat pump. The system was tested in both winter and summer, and parametric studies were done to improve its performance. The results obtained were promising, as the system was able to keep the spaces in the considered comfort zone for the majority of the time (less than 2% of discomfort hours in the winter, and less than 10% in the summer in Lisbon). A modification in the location of the system was also done, from Lisbon to Madrid.

Key Words— energy, Solar energy, Heat pump, Space heating and cooling, Simulink

1. Introduction

1.1 Motivation

The energy sector is currently suffering significant changes to mitigate the climate change and the increase in carbon emissions. Decreasing the energy consumed and the fossil fuel utilization, besides increasing the share of renewable energy sources, are the main modifications necessary in this sector. Buildings are one of the main consumers of energy, representing 40% of the final energy consumption in Europe and 30% in Portugal [1]. The main energy consumed in buildings is used for the heating/cooling of spaces and water heating. For the next years, national and international plans support the reduction of energy consumption in buildings, the increase of the share of renewable energy, as well as the nearly zero energy building (nZEB) concept. nZEB are buildings with high energy performance, in which the low energy consumed must originate mainly from renewable energy sources. The objective of this thesis is to develop a thermal model in Simulink for heating/cooling that integrates renewable energy in a building at Laboratório Nacional de Energia e Geologia (LNEG). This thesis is incorporated in the IMPROVEMENT project, which aims at converting public buildings in nZEB using microgrids. Microgrids are local energy systems that integrate energy generation sources and loads and can be disconnected from the grid, operating independently, being important to incorporate renewable energy.

2. Background

2.1 Solar assisted heat pumps

Solar assisted heat pumps (SAHP) are systems that integrate solar thermal systems and heat pumps. Due to the advantages compared to both technologies separated, they have increased importance in the last years. SAHP can be direct (DX-SAHP)

and indirect (IDX-SAHP), and IDX-SAHP are divided into Series, Parallel, and Dual Source Heat Pumps.

The previous configurations can be combined or new elements can be added to create more complex systems. The use of two tanks has been a common increase in the complexity of the system in the literature found. For example in [2], a system with two tanks was studied, one for domestic hot water (DHW) use and a Float Tank.

Regarding the use of SAHP for space heating, [2] studied a SAHP system with two tanks. The heat pump was used to heat one of the tanks, which is then connected to a radiator. The study concluded that an energy saving of 20% could be achieved if this system was used as a retrofit in the existing Canadian houses. [3] used a system with a water-water heat pump, solar collectors, auxiliary heaters, and two tanks, one of them a seasonal one. The study showed that the solar fraction of the system could be improved when a heat pump is incorporated into the system.

The combination of solar thermal and air-water heat pumps (AWHP) for space heating has been analyzed in several studies to combine solar and atmospheric heat. [4] studied a system in which an AWHP and a solar collector were connected in parallel to a buffer tank. As the solar system could not satisfy the total energy demand, the AWHP was activated when the solar radiation was low. [5] investigated a system with solar collectors and an AWHP. This system could load the tank or provide direct space heating. As an auxiliary heating source, an electrical heater was used when the heat pump could not reach the necessary temperature. The study focused on the effect of component properties on energy demand, analyzing, for example, the effect of the size of the tank and solar heat exchanger on the electricity used.

2.2 Modeling

Different software tools are available and used for the modeling of energy systems. TRNSYS is the most common software for

modeling SAHP and its performance, being other software Energy-Plus, ESP-r, Insel, and Matlab [6]. POLYSUN is also one of the most used commercial software and has already been validated in the literature [7], therefore it was used as validation software for this work.

Matlab/Simulink allows the implementation of a dynamic approach using modular systems. This flexibility is very useful because the system can be divided into modules representing each component, with the equations easily modeled using blocks or code. Matlab includes other useful functionalities for the visualization of the results and offers the possibility of future expansion of the systems [8]. TRNSYS only has simple controllers, which can be a disadvantage. As Matlab/Simulink offers the possibility to create models, both for components and complex control, it was the chosen software.

Solar thermal systems coupled with heat pumps for space heating were already modeled in Matlab/Simulink. [9] modeled a space heating system with a water-water heat pump and fan coils to transfer the heat from the water to the building. However, a gap in the literature was found for models coupling solar thermal and air-water heat pumps for space heating in Matlab/Simulink, being these systems already modeled in TRNSYS [10].

2.3 Control

Different strategies are available to control energy systems. Two of the most used in the literature are the on-off control, and the Model Predictive Control (MPC).

In on-off control, the controlled variable can only have two values: zero or its maximum value. This control strategy has advantages compared to other strategies, such as its simplicity [11]. However, it lacks the accuracy and efficiency of more advanced methods. Several studies found in the literature used on-off control, such as [10] that applied this strategy to control the three pumps of the system. The decision was made based on temperature differences in specific points.

Model Predictive Control is a more advanced control strategy. Its principle is based on the optimization of the system, using a cost function, taking into account future predicted variables. This control strategy has several advantages, both related to control parameters (transient and steady response, multivariable control) and to the prediction of future control actions. According to [11], the main disadvantages are the difficulty to create an accurate model to represent the system, and the cost of the installation. [12] used MPC to control the pumps of a solar HVAC system. The criteria used for the optimization problem were the reduction of the energy consumed by the pumps and proximity to the desired temperature differences.

3. Case Study

The case study of this thesis is a part of a building of Laboratório Nacional de Energia e Geologia (LNEG). In this building, a thermal system to provide heat/cold and an electrical system are installed. This thesis focused on the modeling of the thermal system, together with the building studied.

Figure 1 represents the building simulated in this thesis, which has five rooms, and an unconditioned area that was not modeled. Room 1 is a multiuse room with $80m^2$, Room 2 ($22m^2$) is used for meetings and Rooms 3, 4, and 5 are

individual offices, each with $11m^2$. It was considered that Room 1 had an occupation of eight people and Room 2 five people.

Regarding the exterior walls, the overall heat transfer coefficient was assumed to be between $0.5 - 1 W/m^2K$ and for the interior walls, the overall heat transfer coefficient considered was $0.5W/m^2K$.

The system modeled in this thesis consisted of two solar collectors (with $2 m^2$ each), a 300L tank, an air/water Heat Pump, a 1000L storage tank, and fan coils.

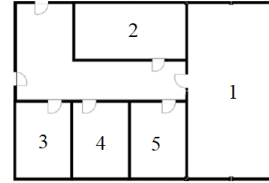


Figure 1 - Part of the building in LNEG studied, Adapted from [13]

4. Methodology and Modeling

4.1 Validation of the solar collector and tank

4.1.1 – Initial model

To simulate the thermal system of LNEG Pilot Plant, previous models of the solar collector and tank developed by [13] were used. These models required validation, to guarantee an accurate performance. The equations of these models are represented in Equations 4.1 to 4.3 and represent a system with a solar collector connected by a pump to a tank with a coil heat exchanger, one entry and one exit. When the pump is on, flowrate circulates in the system, going through the solar collector and the coil. The nomenclature used in the equations throughout this document is presented in the appendix.

$$\rho c_p V \frac{dT_{cout}}{dt} = A_c \eta_0 I - U_{L1} A_c \left(\frac{T_{cout} + T_{cin}}{2} - T_a \right) - U_{L2} A_c \left(\frac{T_{cout} + T_{cin}}{2} - T_a \right)^2 + \rho c_p \dot{V}_c (T_{cin} - T_{cout}) \quad (4.1)$$

$$\rho c_p V \frac{dT_{tout}}{dt} = \rho c_p \dot{V}_t (T_{tin} - T_{tout}) - U_{coil} A_{coil} (T_{tout} - T_{cin}) \quad (4.2)$$

$$\rho c_p V \frac{dT_{cin}}{dt} = \rho c_p \dot{V}_c (T_{cout} - T_{cin}) - U_{coil} A_{coil} (T_{cin} - T_{tout}) \quad (4.3)$$

With y_i being the variable considered in Polysun and \hat{y}_i in Simulink.

4.1.2 – New model

As will be discussed in Chapter 5, the model described above presents some limitations and changes were performed that are described below.

Solar collector

The temperature of the collector used to account for the losses to the atmosphere was changed, in the validation process, with respect to Equation 4.1. The expression used in the models for the calculation of the temperature at the inlet of the solar collector is an energy balance at the exit of the coil of the tank. This aspect does not have implications when the pump is on, as there are no significant differences between the temperature at

these two locations (exit of the coil of the tank and inlet of solar collector). However, when the pump is off, T_{cin} is calculated as being in contact with the tank, and therefore, is at a temperature close to the temperature of the tank. As the temperature of the tank is usually high, the average between the T_{cin} and T_{cout} (in contact with the solar collector) becomes high as well, increasing the losses of the solar collector to the atmosphere. However, the losses in the solar collector, are not able to decrease the temperature at the tank, keeping T_{cin} at the same values, despite the losses in the solar collector. This effect brings T_{cout} to significantly low temperatures, as the losses are oversized. A different equation was considered when the pump was off, to eliminate this problem. The final equation for the solar collector model when the pump is off is,

$$\rho c_p V \frac{dT}{dt} = A_c \eta_0 I - U_{L1} A_c (T_{cout} - T_a) - U_{L2} A_c (T_{cout} - T_a)^2 + \rho c_p \dot{V}_c (T_{cin} - T_{cout}) \quad (4.4)$$

Tank

The new model accounts for the stratification of the tank, considering 12 layers, as it is the number of layers considered in POLYSUN. In a stratified tank, the layers at the top have a higher temperature than the layer at the bottom. In the Simulink model, the stratification effect was simulated based on [14]. If any layer at any time had a temperature higher than the layer above or lower than the layer below, a tunable constant Δ was set from zero to a value of a high order of magnitude to transfer the heat upwards and correct the situation.

The coil considered is in the middle of the tank (Layer 5 to 8). The water demand leaves the tank in layer 1 and returns cold to layer 12. When the flowrate that leaves the tank is different from zero, the model considers that every layer receives a flowrate from the layer below.

As the coil is in contact with layers at different temperatures, it was separated into four equal parts, each in contact with one layer. A term accounting for losses was added to the Simulink model, as it is considered in POLYSUN. The final equations of the system based on [15] and [14] are summarized in Table 1.

Table 1 - Equations for the temperature in each layer of the tank

Temperature in the layer	Equation
1	$\rho c_p V_{tank} \frac{dT}{dt} = \rho c_p \dot{V}_t (T_{j+1} - T_j) - \dot{Q}_{loss} + \dot{Q}_{c1} \quad (4.5)$
2-4,9-11	$\rho c_p V_{tank} \frac{dT}{dt} = \rho c_p \dot{V}_t (T_{j+1} - T_j) - \dot{Q}_{loss} + \dot{Q}_{c1} + \dot{Q}_{c2} \quad (4.6)$
5-8	$\rho c_p V_{tank} \frac{dT}{dt} = \rho c_p \dot{V}_t (T_{j+1} - T_j) - \dot{Q}_{loss} + \dot{Q}_{c1} + \dot{Q}_{c2} - \dot{Q}_{coil} \quad (4.7)$
12	$\rho c_p V_{tank} \frac{dT}{dt} = \rho c_p \dot{V}_t (T_{in} - T_j) - \dot{Q}_{loss} + \dot{Q}_{c2} \quad (4.8)$

$\dot{Q}_{coil} = U_{coil} A_{coil} (T_j - T_{cini})$ is the heat transferred in the coil, $\dot{Q}_{loss} = U_{loss} A_{loss} (T_j - T_a)$ the heat lost to the atmosphere, $\dot{Q}_{c1} = \frac{k_{j1} \Delta c}{\Delta x} (T_{j+1} - T_j)$ the heat exchange by conduction with the lower layer, $\dot{Q}_{c2} = \frac{k_{j2} \Delta c}{\Delta x} (T_{j-1} - T_j)$ the heat exchange by conduction with the upper layer. The variables k_{j1} and k_{j2} are the thermal conductivity and are represented in Equations 4.9 and 4.10. These variables are equal to the thermal conductivity of the water when the tank is stratified. However, when the tank is not stratified, they are given by the conductivity of the water times a tunable parameter and a difference of temperature (model from [14] to correct the stratification).

$$k_{j1} = \begin{cases} k_{j1} \Delta |T_{j+1} - T_j| & \text{if } T_j < T_{j+1} \\ k_{j1} & \text{else} \end{cases} \quad (4.9)$$

$$k_{j2} = \begin{cases} k_{j2} \Delta |T_{j-1} - T_j| & \text{if } T_j < T_{j-1} \\ k_{j2} & \text{else} \end{cases} \quad (4.10)$$

Equation 4.11 represents the temperature that returns to the solar collector, which is calculated as in contact with the coil.

$$\rho c_p V_{coil} \frac{dT_{cin(i)}}{dt} = \rho c_p \dot{V}_c (T_{cin(i-1)} - T_{cin(i)}) + \dot{Q}_{coil} \quad (4.11)$$

4.1.3 – Validation procedure

As mentioned before, the software used for the validation was POLYSUN. Two elements were validated together: the solar collector and the tank. The solar collector model used was a flat plate collector, with a volume of 3L and an aperture area of $8m^2$. The tank model used had 500L and coil heat exchanger. The system has a pump with an on-off controller that switches on whenever the outflow temperature of the solar collector is higher than the temperature of the last layer in contact with the fluid in the coil. For the validation process, the weather conditions and the characteristics of the simulated components in both programs were equal. As the source for the weather data in POLYSUN is Meteonorm, the exterior temperature data was downloaded from this source and considered in the Simulink model. Irradiance from POLYSUN accounting for the tilt angle of the solar collector was used as input for Simulink. A typical hot water demand was selected from POLYSUN templates and considered in Simulink, as the solar collector together with the tank without backup is not able to exchange a large amount of energy. The demand profile was an hourly flowrate profile, with a return water temperature of $20^\circ C$. The same heat demand was considered in both software tools.

4.2 Validation of the fan coil

4.2.1 – Initial model

A fan coil is used to exchange heat between the water system and the building. The fan coil model was previously performed by [13] following Equations 4.12 to 4.14.

$$\rho_a c_{p_a} V_a \frac{dT_{aout}}{dt} = \rho_a c_{p_a} \dot{V}_a (T_{ain} - T_{aout}) - U_{fc} A_{fc} (T_{aout} - T_{wout}) - \dot{Q}_{loss} \quad (4.12)$$

$$\rho_w c_{p_w} V_w \frac{dT_{wout}}{dt} = \rho_w c_{p_w} \dot{V}_w (T_{win} - T_{wout}) - U_{fc} A_{fc} (T_{wout} - T_{aout}) \quad (4.13)$$

$$\dot{Q}_{loss} = h A_o (T_{aout} - T_{building}) \quad (4.14)$$

4.2.1 – New model

Analyzing the equations and the results from POLYSUN, a better agreement with the software results was achieved by considering some modifications. These modifications included changes in the average temperature of the air for losses and the use of the log mean temperature. The log mean temperature was applied to calculate the heat transferred in the fan coil, as it was considered that the fan coil was a heat exchanger. The final model of the fan coil is represented by the following equations:

$$\rho_a c_{p_a} V_a \frac{dT_{aout}}{dt} = \rho_a c_{p_a} \dot{V}_a (T_{ain} - T_{aout}) + UA \Delta T_{lm} - \dot{Q}_{loss} \quad (4.15)$$

$$\rho_w c_{p_w} V_w \frac{dT_{wout}}{dt} = \rho_w c_{p_w} \dot{V}_w (T_{win} - T_{wout}) - UA \Delta T_{lm} \quad (4.16)$$

$$\Delta T_{lm} = \frac{\Delta T_1 - \Delta T_2}{\ln(\Delta T_1 / \Delta T_2)} \quad (4.17)$$

$$\Delta T_1 = T_{hi} - T_{co} = T_{win} - T_{aout} \quad (4.18)$$

$$\Delta T_2 = T_{ho} - T_{ci} = T_{wout} - T_{ain} \quad (4.19)$$

$$\dot{Q}_{loss} = hA_o \left(\frac{T_{ain} + T_{aout}}{2} - T_{building} \right) \quad (4.20)$$

4.2.3 – Validation procedure

The system created in POLYSUN is displayed in Figure 2. This system consists of the solar collector and tank previously validated, a fan coil, and a building. The nominal air and water flowrates in the fan coil model of POLYSUN were 42l/s and 73l/h respectively, which values were also considered for the Simulink model. The pump between the fan coil and the tank had a constant flowrate always circulating. The system implemented in Simulink is represented in Figure 3.

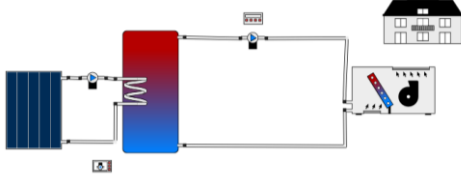


Figure 2 - Thermal system made in POLYSUN

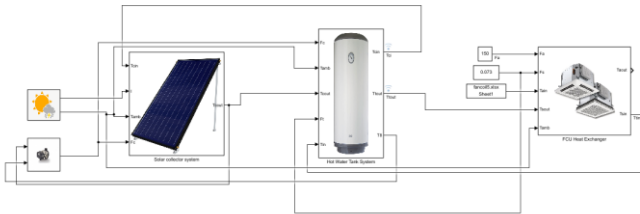


Figure 3 - Thermal system made in Simulink/Matlab for validation

4.3 Heat Pump

For the model of the heat pump, two options are available: empirical and mathematical models. An empirical model was considered in this thesis, as the mathematical model is too complex for the purpose of this study and required information that is not available. The information required for the empirical model, such as the heat transferred (power of the heat pump)

and the electrical power for different conditions, was obtained from a datasheet provided by the manufacture.

The empirical model was done in Simulink. For each state (water and air temperature), the heat and electrical power of the heat pump were interpolated from the datasheet values.

The datasheet had the parameters of the heat pump for a fixed water temperature difference (between the inlet and outlet of the heat pump) of 5°C. Consequently, the water flowrate circulating through the heat pump changes with the temperatures in the heat pump, and therefore it is also calculated in the model.

4.4 Global system

The global system simulated in this work is represented in Figure 4. The configuration in winter and summer has some important differences. In winter, the solar collector is connected to the hot water tank by a solar system pump, while in summer the connection of the solar collector to the system is switched off. The water leaving the hot water tank can flow, in both seasons, directly to the storage tank, passing through the tank pump, or can flow through the heat pump where extra heat/cold is given. After that, the water leaves the storage tank to exchange heat with air from the rooms, through the five fan coils, returning then to the tank. The difference between seasons in this process is the position of extraction from the tanks. In winter, the water leaves the tanks at the top layer and returns to the bottom layer, whereas in the summer the direction changes, as the goal is to cool the space and have low temperature in the tanks.

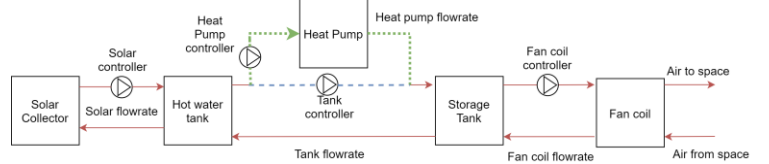


Figure 4 - Configuration of the global thermal system simulated

To model the system from LNEG Pilot plant, the characteristics of the individual models already validated had to be adapted. The parameters of the solar collector in LNEG are listed in Table 2.

Table 2 - Characteristics of the elements of the thermal system in LNEG

Solar collector			Hot water tank	Storage tank
η_o	0,770	V	0,300 m ³	1,00 m ³
U_{L1}	3,50 W/m ² K	V_{coil}	0,0101/8 m ³	0,0193/8 m ³
U_{L2}	0,0170 W/m ² K	U_{coil}	250 W/m ² K	250 W/m ² K
A	2,00 m ²	A_{coil}	1,50/8 m ²	2,70/8 m ²
V	0,00190 m ³	U_{loss}	0,500 W/m ² K	0,250 W/m ² K

The location of the coil in the hot water tank of the Pilot plant is slightly different from the one modeled, as it is in contact with the middle and bottom layers. The storage tank has the same configuration as the hot water tank. The properties of the two tanks are presented in Table 2. It was considered that both tanks were installed in a room with a fixed temperature of 20°C.

Three different sizes of the fan coil were modeled to satisfy the necessities of the three types of spaces. A typical medium fan

coil was chosen for the Room 2 based on catalog data found, and the size and flowrate of the other fan coils were determined based on an extrapolation procedure, accounting for the respective dimensions of the spaces. For Room 1, 950 m^3/h of air were considered, 250 m^3/h for Room 2, and 125 m^3/h for Rooms 3, 4, and 5.

4.5 Building

The model used for the building in this thesis was based on [13], which is described by the following equation:

$$\rho c_p V_i \frac{dT_i}{dt} = \rho c_p \dot{V}_{HVAC} (T_{aout(i)} - T_i) - U_{ext} A_{ext} (T_i - T_a) - \sum_{i=1}^{N_r} U_{int} A_{int} (T_i - T_k) + \rho c_p \dot{V}_{vent} (T_a - T_i) + \dot{q} \quad (4.21)$$

The equation represents the energy balance of the space. The accumulation of energy in the space depends on the heat transferred by the fan coil, the heat exchanged between the room and the exterior and the room and the other rooms in contact with it, the ventilation of new air, and the heat generation inside the room.

The necessary flowrate of new air was considered to be 24 m^3/h per person, as suggested in [16].

4.6 On-Off Control

Regarding the control strategy, the on-off control was implemented in the eight pumps of the system, based on specific temperatures or differences between temperatures. For the winter season, the criteria used to control the pumps are listed in Table 3 and Table 4. The solar system pump is controlled based on the temperature difference between the outflow water of the solar collector and the bottom layer of the tank (last layer in contact with the coil). The same procedure was applied for the control of the tank pump, in this case using the difference between the temperature at the exit of the hot water tank and the bottom temperature of the storage tank. The reference temperature for the storage tank was set to 50°C and the difference between this reference temperature and the outflow temperature of the storage tank was used as the control variable for the heat pump. The heat pump only switched on if the hot water tank had the capacity to heat the storage tank. A minimum operation time of 0.1hour (6minutes) was set for all the pumps in the system to prevent frequent switching off, except for the pumps of the fan coils, where the operation time was not limited.

Table 3 - Criteria to switch on-off the pumps of the system

	Solar system pump controller	Tank pump controller	Heat pump controller
On	$T_{cout} - T_{12} > 5^\circ\text{C}$	$T_{tout} - T_{s12} > 5^\circ\text{C}$	$T_{ref} - T_{sout} > 5^\circ\text{C}$
Off	$T_{cout} - T_{12} < 1^\circ\text{C}$	$T_{tout} - T_{s12} < 1^\circ\text{C}$	$T_{ref} - T_{sout} < -1^\circ\text{C}$

The occupation period of the rooms was considered between 8 am and 7 pm when the control follows the equations listed in Table 4. The system heated the spaces before the occupants arrive (6 am-8 am) and from 7 pm to 6 am, the comfort in the space was relaxed.

Table 4 - Criteria to switch on-off the heating of the rooms

	8am – 7 pm	6 am – 8 am	7pm – 6 am
On	$T_{space} < 21^\circ\text{C}$	$T_{space} < 18^\circ\text{C}$	$T_{space} < 15^\circ\text{C}$
Off	$T_{space} > 24^\circ\text{C}$	$T_{space} > 22^\circ\text{C}$	$T_{space} > 22^\circ\text{C}$

Regarding the summer season, the solar system pump is always off and the tank and heat pump controllers have the same conditions of switching on and off as in the Winter. The differences are the signal of the left terms in Table 3 and the layer of the storage tank used for the tank pump controller, which was the last one in contact with the fluid in the coil (Layer 5). The chosen reference temperature for the heat pump in the summer was 10°C. When the temperature of the hot water tank reached 7°C, the heat pump was switched off, to prevent too low temperatures in the hot water tank.

The conditions used for the controller of the building are represented in Table 5. From 7 pm to 6 am, the cooling of the space is switched off because the low exterior temperatures at night help to decrease the temperature of the space. For the period between 6 am and 8 am, the same principle used in the winter is applied.

Table 5 - Criteria to switch on-off the cooling of the rooms

	8am – 7 pm	6 am – 8 am	7pm – 6 am
On	$T_{space} > 24^\circ\text{C}$	$T_{space} > 26^\circ\text{C}$	-
Off	$T_{space} < 21^\circ\text{C}$	$T_{space} < 23^\circ\text{C}$	-

4.7 Model Predictive Control

For the solar system pump, a new control strategy was implemented, in this case, Model Predictive Control (MPC). The decision of the value of the solar system flowrate (\dot{V}_c) (either zero or its maximum value) is done based on an optimization cost function, which receives information from a linear model of the system studied, as represented in Figure 5. In the linear model, the system with the solar system pump on and off is simulated for each time with the correspondent irradiance, ambient temperature, and the previous variables from the system. The temperature at the top layer of the hot water tank, for both options (on and off of the pump), is the output of the linear system and the input of the optimization problem. For simplification, the system is optimized based on the best option for the current time step, not using the prediction of disturbances, as typically done in MPC.

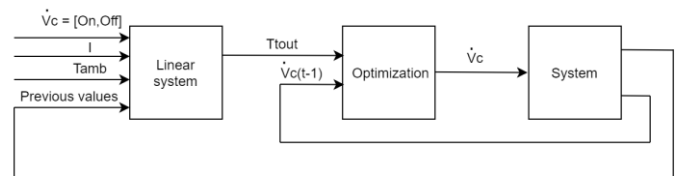


Figure 5 - Process used to apply MPC in the thermal system

In order to have a linear model of the system to apply MPC, a linearization procedure was implemented through linear

equations. A simpler model was created with only the solar collector and the hot water tank connected, for the linear model of the system. This simplified model was run several times, with different parameters (see Table 6), simulating a period of 30 minutes each time.

Table 6 - Values used for the linearization of the system

	Values	Units
Solar system flowrate	[0,0.288]	m^3/h
Outflow temperature Solar collector	[10,30,50,70,90]	$^{\circ}C$
Temperature of the tank	[10,30,50,70,90]	$^{\circ}C$
Irradiance	[0,50,250,500,1000,1500]	W/m^2
Ambient temperature	[5,15,25]	$^{\circ}C$
Flowrate between tanks	[0,2,3,4]	m^3/h
Water return temperature to the HW tank	[20,35,50]	$^{\circ}C$

The output of the system (T_{tout}) was saved for each simulation, and a linear regression calculation function from Matlab was used following Equation 4.22 with $t-1$ representing the previous value, \dot{V}_t the flowrate between tanks and T_{tin} the return water temperature to the hot water tank.

$$T_{tout} = a_1 I + a_2 T_a + a_3 T_{tout(t-1)} + a_4 T_{tin(t-1)} + a_5 \dot{V}_{t(t-1)} + a_6 \quad (4.22)$$

The data was divided into specific conditions as the dynamic of the system in these cases changed significantly. The following conditions were used:

- T_{cout} is higher or lower than T_{tout} ($\Delta T > 0$ or $\Delta T < 0$);
- Irradiance is zero (night), or different from zero (day);
- Flowrate between the tanks and the solar system flowrate are zero or not.

These options were divided into 4 cases, listed in Table 7. Each case was then divided into four more cases, each one for a specific value of the two flowrates.

Table 7 - Cases used for the linearization of the thermal system

Case	ΔT	I
1	< 0	$= 0$
2	> 0	$= 0$
3	> 0	$\neq 0$
4	< 0	$\neq 0$

The optimization problem consisted of a cost function (Equation 4.23) that penalized the option (zero or maximum flowrate) that had a higher difference to the reference value and higher changes of flowrate with time (to prevent damage on the pump). s_1 and s_2 are used to create dimensionless terms, being considered equal to the maximum amplitude of the signals. The reference temperature for the MPC controller considered was $85^{\circ}C$ because it is close to the maximum temperature allowed in the tank ($90^{\circ}C$). w_1 and w_2 are the weights of each term.

$$f(x) = \left(\frac{w_1}{s_1} (T - T_{refmpc}) \right)^2 + \left(\frac{w_2}{s_2} \Delta \dot{V} \right)^2, \quad (4.23)$$

$$\Delta \dot{V} = \dot{V}_{c(t)} - \dot{V}_{c(t-1)}$$

5. Results

5.1 Validation of the solar collector and tank

For a numerical comparison between POLYSUN and Simulink models, the root mean square error (RMSE) was applied, which is defined as:

$$RMSE = \sqrt{\frac{1}{n} \sum_{i=1}^n (\hat{y}_i - y_i)^2} \quad (5.1)$$

Even after the modifications in the solar collector, the validation showed poor results for the temperature in the tank, with significantly higher temperatures than in POLYSUN, even adding losses to the tank. The Simulink model developed by [13] for the tank simulated only the volume of the layers in contact with the coil heat exchanger, as a simplification to the model. This approach is not considered in POLYSUN, which models a stratified tank. Therefore, a new model of the tank was developed in Simulink.

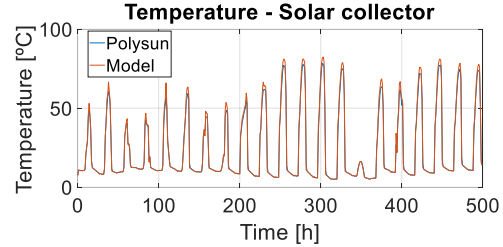


Figure 6 - Outflow temperature of the solar collector of POLYSUN and Simulink

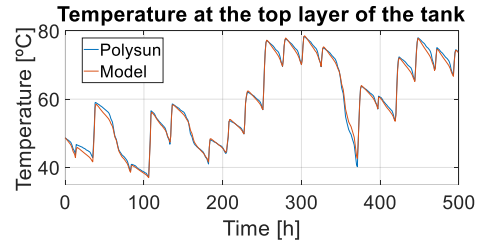


Figure 7 - Temperature in the tank of POLYSUN and Simulink

Table 8 - Error metric of the validation of the tank and solar collector

	RMSE
T1 ($^{\circ}C$) - Top Layer	1,05
T5 ($^{\circ}C$)	3,00
T8 ($^{\circ}C$)	2,08
T9 ($^{\circ}C$)	2,16
Tcout ($^{\circ}C$)	2,38
Tcin ($^{\circ}C$)	5,49
Qcollector (W)	69,6

The comparison between the results of the new model in Simulink and POLYSUN is presented in Figures 6 and 7. The period selected for the graphs considered corresponds to a part of January. The models showed very accurate results, reproducing POLYSUN. The outflow temperature is sometimes overestimated, with a maximum deviation of 29% in the periods of highest irradiance. This effect could be explained by differences in the equations used in POLYSUN, by differences in the calculation method for the coil used in POLYSUN, by minor effects that were not modeled in Simulink (losses in connections, exits, and pump), as well as by the propagation of small errors. In addition, the exact location of the variable T_{cin} in the tank in POLYSUN is not known. Regarding the hours that the solar system flowrate switches on or off, some differences appeared in the comparison of the outflow temperature of the solar collector between the two

software tools. This effect can be explained by small differences between T_{cout} and T_8 in both programs. The error metric of the comparison between the results of the two software tools is presented in Table 8, following equation 5.1. As indicated, the errors are small, confirming the accuracy of the model implemented.

5.2 Validation of the fan coil

The initial model of the fan coil showed significant differences with respect to the POLYSUN output. Better results were observed with the new model.

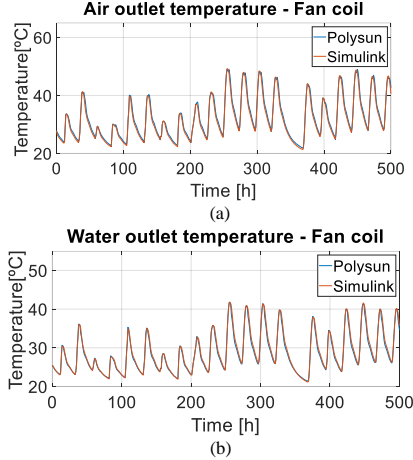


Figure 8 - Comparison between the fan coil of POLYSUN and Simulink, a) Air temperature, b) Water temperature

Table 9 - Error metric of the validation of the fan coil

	RMSE
T_{aout} (°C)	0,996
T_{wout} (°C)	0,705
T_1 (°C)	0,475
Q_{fc} (W)	22,9
T_{cout} (°C)	1,79
$Q_{collector}$ (W)	46,2

The results illustrated in Figure 8 (Air and water outflow temperature) and Table 9 showed that the new model implemented in Simulink reproduces, with high accuracy, the system in POLYSUN. The differences obtained could be associated with error propagation.

5.3 Comparison of on-off Control and Model Predictive Control

As explained in Chapter 4, to apply MPC to the system, a linear model was developed. The linearization of the system with the cases specified in Chapter 4 Table 7 provided good results, as all the linear regressions had values of $R^2 > 0.9995$. Considering the difference between the value of T_{tout} obtained with the model and the linearization, the highest error was equal to 3.122% and happened in case 3 with solar system flowrate and flowrate between tanks.

The first comparison, with $w_1 = 1$ and $w_2 = 0.1$, showed that the temperature of the storage tank with the MPC was lower than the one from On-Off in the first days, being the comparison not straight after some days. However, the system did not have constant switching off during the operation. The on-off has a very frequent switching of the pump that can be explained by

the term $\rho c_p \dot{V}(T_{cin} - T_{cout})$ in Equation 4.1 starting to have values different from zero when the system begins to have solar flowrate, decreasing rapidly the temperature.

As with $w_2 = 0.1$ the flowrate does not switch off during operation, it could indicate that excessive importance is given to the variation of the flowrate. To study the effect of w_2 on the system and in an attempt to improve the performance of the MPC controller, the weight of the variation of flowrate w_2 was decreased. w_2 defines the importance that the system gives to the variation of the flowrate. Therefore decreasing the weight decreases the importance given and the solar system pump may switch off more frequently during operation.

The most favorable result was found with $w_2 = 0.01$ (see Figure 9), where the temperature in the tank is practically equal to the one obtained with on-off control. Although the MPC controller has instants when the pump switches off during operation, this effect is always single (in contrast to the on-off control that, on the same day, switches on and off the pump several times). The control method does not have a significant impact on the temperature of the rooms and on the comfort. The chosen control for the winter was MPC with a weight of 0.01 as it reaches a closer tank temperature to the one from on-off and switches off less frequently during operation.

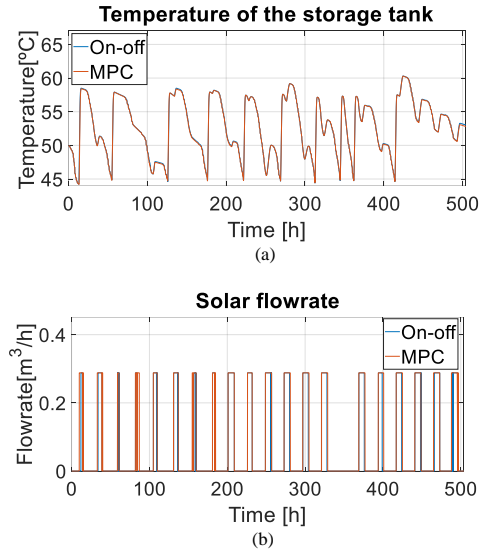
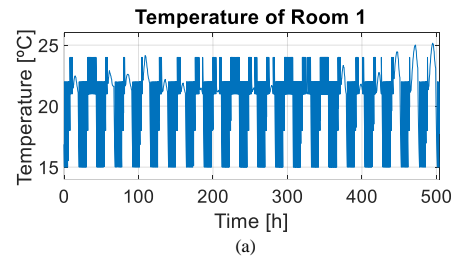


Figure 9 - Comparison between On-off and MPC control for $w_2 = 0.01$, a) Temperature of the storage tank, b) Solar system flowrate

5.4 System with Model Predictive Control – Winter



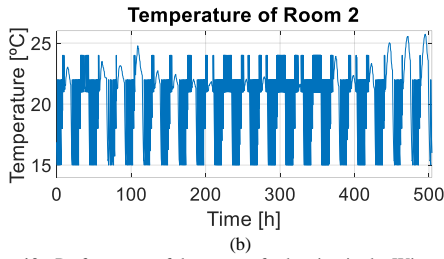


Figure 10 - Performance of the system for heating in the Winter, a) Temperature of Room 1, b) Temperature of Room 2

The temperature of Room 1 and Room 2 are represented in Figure 10. It was considered that the space is out of the comfort zone if $T_{space} > 25^{\circ}\text{C}$ or $T_{space} < 20^{\circ}\text{C}$, both in the winter and in the summer. The system is able to provide heat for all the rooms, keeping the system in the comfort zone for the majority of the time. Rooms 1,2 and 5 have an excess of loads, and therefore do not need heat on some days during the occupation period. The heat consumption in Room 3 is higher than in Room 4 and 5 as it has a larger area in contact with the exterior for the same occupation. During the three weeks studied, the heat pump switches on 11 times, consuming 122,9 KWh.

5.5 System with On-Off Control – Summer

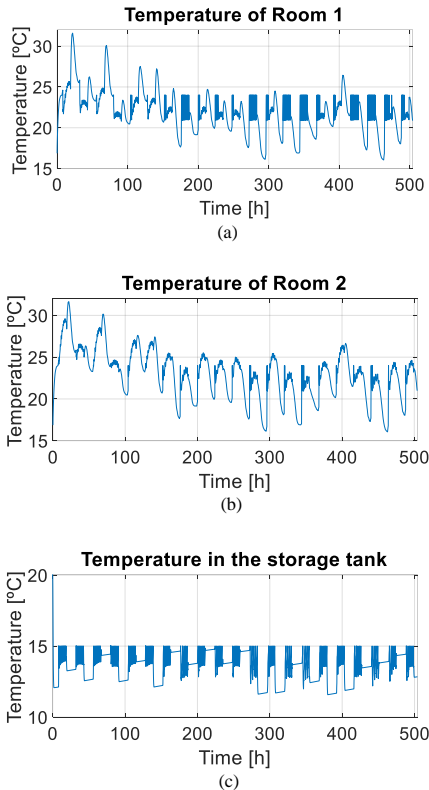


Figure 11 - Performance of the system for cooling in the Summer, a) Temperature of Room 1, b) Temperature of Room 2, c) Temperature in the storage tank

Figure 11 shows the performance of the system in the summer. The temperature of the rooms during the occupation time is in the comfort zone for the majority of the time. Room 2 is the space with the worst cooling performance, with 13,15% of the occupation time out of the comfort zone, due to an excess of thermal loads in the room. Room 3 is the second room with more discomfort, which can be possibly explained by the fact

that this room has a higher area in contact with the exterior than the other rooms of the same size. The discomfort hours in Rooms 1, 4, and 5 are not significant. As mentioned in Chapter 4, the system does not have any cooling between 7 pm to 6 am. During the night, the only heat exchanged in the room is the heat transfer through the exterior and interior walls, which brings the temperature of the space close to the exterior ambient temperature. As in the summer, the ambient temperature at 7 pm can still have high values, there is an increase in temperature of the rooms after the cooling is switched off at those hours, reducing then during the night. The temperature of the storage tank is most of the time equal to or lower than 15°C because the heat pump is controlled to switch on when the temperature of the tank is 5°C higher than the reference (in this case 10°C). The heat pump switches on and off every day and several times within the day, consuming 150,5 KWh of electric energy.

5.6 Parametric Studies

Having the behavior of the system in the winter and the summer for some specific conditions, parametric studies can be performed to investigate the influence of relevant parameters of the system. To compare the performance of each study, three main variables were analyzed: the number of hours in discomfort during the occupation time (8 am-7 pm), the product of the difference of the temperature of the space to the comfort zone and the time period out of the comfort zone (degree.hour of discomfort), and the electric energy used in the heat pump. The period of study was three weeks, both in the winter and summer, in order to have enough information without a large computational time.

5.6.1 Study 1: Heating during the night – Winter

The focus of this study is the heating of the spaces during the night in the Winter, and its influence on the comfort and electric energy consumed by the heat pump. The initial condition consisted of heating the space when the temperature was below 15°C and until it reached 22°C . To vary this parameter, three other options were studied: always switching off the heat during the night, heating between 15°C and 18°C , and between 18°C and 22°C . The results showed that the four options have a similar percentage of discomfort hours and a similar degree.hours discomfort. The hours of discomfort are, in the majority of the time, when, at 8 am (beginning of the occupation time), the system was at a temperature below 20°C , reaching rapidly the temperatures of comfort. The other type of discomfort is due to an excess of loads in the rooms, which brings the temperatures of the rooms to values above 25°C . This effect causes the majority of the discomfort in Room 2, which is the room with more discomfort hours (approximately 1.7%). The electric energy consumption in the heat pump changes significantly between the cases considered, with the off option using less than half of the energy of the two last cases (60,08 KWh with Off and 143,4 KWh with 18/22°C). This difference in the electric energy consumption of the heat pump can be explained using Figure 12. This temperature decreases faster when the heating is on at night as it exchanges energy with the rooms, decreasing the temperature of the water that returns to the storage tank. Off was the chosen option as it uses less electrical energy and does not increase significantly the discomfort hours and the discomfort temperature.

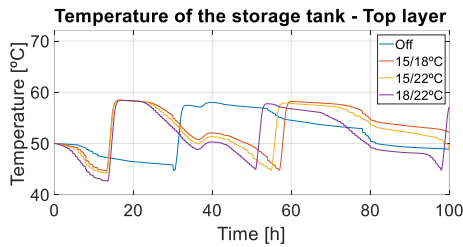


Figure 12 - Temperature of the storage tank for the cases in Study 1

5.6.2 Study 2: Location – Winter

The system was simulated in Madrid as it has a lower ambient temperature in the winter. The results showed that the heat needed in Madrid is higher, leading to a faster decrease of the temperature in the storage tank, to a higher switching frequency of the heat pump, and to a higher electric heat pump energy consumption (219,1 KWh in Madrid comparing with 60,08 KWh in Lisbon). The discomfort hours decreased (0,06% in Madrid and 1,69% in Lisbon in Room 2), as some of these periods were related to an excess of internal loads in Lisbon. The degree.hours in discomfort periods decreased or was at similar levels to Lisbon for all the rooms.

In Madrid, the loads generated inside the building are compensated with higher losses to the outdoor and lower temperature of the inlet atmospheric air, which decreases the excess of loads, increasing the heat needed. The system in Madrid required a more frequent usage of the heating.

5.6.3 Study 3: Solar collector area - Winter

It is expected that the increase of the solar collector area would increase the amount of energy transferred to the fluid and the useful heat in the solar collector. With this effect, the temperature of the tank increases, requiring less energy from the heat pump. The area of the solar collector was increased by a factor of two, from 4 to 8m², to analyze the impact on the system. The results are as expected, with the system decreasing the electric power needed and absorbing more solar energy. The electric energy consumed by the heat pump is reduced from 61,39KWh to 36,88 KWh (60% less) when the solar collector area is increased from 4 to 8m². The comfort does not change significantly between the two cases.

5.6.4 Study 4: Reference temperature – Summer

The reference temperature is a parameter of the heat pump controller that is used to decide when to switch on or off the heat pump, as explained in Chapter 4. This parameter influences the temperature of the storage tank, which influences both the discomfort in the building and the electric power used in the heat pump. The reference temperatures analyzed were 8°C, 10°C (initial condition), and 15°C. Due to a fast reach of significantly low temperatures at the outlet of the heat pump, lower reference temperatures were not studied. The system with a reference temperature of 8°C has lower discomfort hours (2,6% of the hours of occupation with a reference temperature of 8°C in discomfort, 4,2% with 10°C, and 15% with 15°C) and lower degree.hours in discomfort. This happens because the temperature in the storage tank increases as the reference temperature increases (see Figure 13). The electric energy used by the heat pump for the system with a reference temperature

of 8°C is only 5% higher than the one with 10°C as reference temperature while reducing the discomfort in all the rooms by 62% on average. Therefore, a reference temperature of 8°C was chosen as the best scenario.

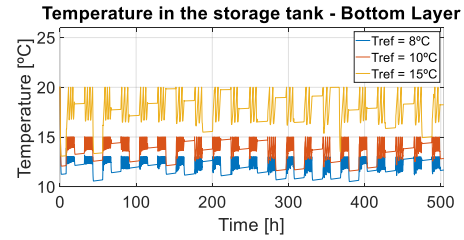


Figure 13 - Evolution of the temperature in the storage tank for the three cases in Study 4

5.6.5 Study 5: Location – Summer

In order to study the influence of the weather in the Summer, the system location was changed to Madrid, that according to the data from POLYSUN, has a higher ambient temperature than Lisbon in the summer. As expected, Madrid has more discomfort hours in all the rooms (27% of discomfort hours in Room 2 compared to 9,0% in Lisbon), with an increase in the degree.hours of discomfort. This effect can be explained by the importance of the ambient temperature in the loads of the building (losses to the exterior and ventilation). Regarding the electric energy consumed by the heat pump, Madrid needs more 43% than Lisbon, due to higher instant power and to a higher frequency of switching on the heat pump.

5.6.6 Study 6: Occupation of Room 2 - Summer

Room 2 is the room with more discomfort in the summer. A parametric study was done where the occupancy of the room was changed, keeping the occupancy of the other rooms fixed. It was considered that two, three, four, or five people could be in this space (meeting room), being five the value previously used. The number of people was considered fixed for the period of study. We observed that with a lower number of occupants in Room 2, the system is able to bring all the spaces to the comfort zone almost all the time studied (9,0% of discomfort hours with 5 people to 0,88% with 2 in Room 2). This is due to fewer loads in the room, which decreases the amount of cooling needed in the space. This change in the occupation of Room 2 does not have a significant impact on the temperature of the other rooms. The electric energy used by the heat pump reduces as the number of people reduces (10% less with 2 people than with 5), as the loads inside the room decrease, decreasing the temperature of the air and the heat exchanged in the fan coil.

6. Conclusions

This thesis consisted of the modeling of the thermal system located on LNEG Pilot Plant. The first objective was the validation of models of the solar collector, tank, and fan coil, which, after some modifications, was accomplished.

The complete integrated model constituted by a solar collector, two tanks, a heat pump, and fan coils, and with the objective of heating/cooling a building was implemented successfully, filling the gap in the literature found. The system was able to keep the building in its comfort zone for the majority of the

time. Two control strategies were studied, with MPC showing more stable results.

This work showed that Simulink is a suitable software to model thermal systems and their control, due to its flexibility and its adaptability.

This thesis was only focused on the thermal system. An important upgrade would be to consider the integration with the electrical system, having decision making based on both systems. The heat pump is the main component affected by the proposed integration of the two systems, being necessary to develop a new control approach.

Some components of the Pilot Plant in LNEG are still being installed, therefore an experimental study and comparison with the simulated system were not possible. In the future, it would be interesting to compare the simulation results obtained with the experimental data.

A simplified MPC was implemented in this work. To have better results and a better control strategy, an increase of the complexity of MPC would be required, applying modes of prediction of the disturbances (for example weather forecast).

References

- [1] “Edifícios.” <https://www.dgeg.gov.pt/pt/areas-setoriais/energia/eficiencia-energetica/edificios/> (accessed Feb. 15, 2021).
- [2] S. R. Asaee, V. I. Ugursal, and I. Beausoleil-Morrison, “Techno-economic assessment of solar assisted heat pump system retrofit in the Canadian housing stock,” *Appl. Energy*, vol. 190, pp. 439–452, 2017, doi: 10.1016/j.apenergy.2016.12.053.
- [3] M. Pinamonti, I. Beausoleil-Morrison, A. Prada, and P. Baggio, “Water-to-water heat pump integration in a solar seasonal storage system for space heating and domestic hot water production of a single-family house in a cold climate,” *Sol. Energy*, vol. 213, no. October 2020, pp. 300–311, 2021, doi: 10.1016/j.solener.2020.11.052.
- [4] T. Long *et al.*, “Performance analysis and optimization of a solar-air source heat pump heating system in Tibet, China,” *Energy Build.*, vol. 220, p. 110084, 2020, doi: 10.1016/j.enbuild.2020.110084.
- [5] S. Poppi, C. Bales, M. Y. Haller, and A. Heinz, “Influence of boundary conditions and component size on electricity demand in solar thermal and heat pump combisystems,” *Appl. Energy*, vol. 162, pp. 1062–1073, 2016, doi: 10.1016/j.apenergy.2015.10.190.
- [6] J. Vega and C. Cuevas, “Parallel vs series configurations in combined solar and heat pump systems: A control system analysis,” *Appl. Therm. Eng.*, vol. 166, no. May 2019, p. 114650, 2020, doi: 10.1016/j.applthermaleng.2019.114650.
- [7] P. Jelinek, J. Sedláč, and B. Lišková, “Comparison of polysun simulation with direct measurements of solar thermal system in rapotice,” in *Advanced Materials Research*, 2014, vol. 1041, pp. 158–161, doi: 10.4028/www.scientific.net/AMR.1041.158.
- [8] S. Lim, S. Park, H. Chung, M. Kim, Y. J. Baik, and S. Shin, “Dynamic modeling of building heat network system using Simulink,” *Appl. Therm. Eng.*, vol. 84, pp. 375–389, 2015, doi: 10.1016/j.applthermaleng.2015.03.068.
- [9] A. Vallati, P. Ocloñ, C. Colucci, L. Mauri, R. de Lieto Vollaro, and J. Taler, “Energy analysis of a thermal system composed by a heat pump coupled with a PVT solar collector,” *Energy*, vol. 174, pp. 91–96, 2019, doi: 10.1016/j.energy.2019.02.152.
- [10] J. Deng, Z. Tian, J. Fan, M. Yang, S. Furbo, and Z. Wang, “Simulation and optimization study on a solar space heating

system combined with a low temperature ASHP for single family rural residential houses in Beijing,” *Energy Build.*, vol. 126, pp. 2–13, 2016, doi: 10.1016/j.enbuild.2016.05.019.

- [11] F. Behrooz, N. Mariun, M. H. Marhaban, M. A. M. Radzi, and A. R. Ramli, “Review of control techniques for HVAC systems-nonlinear approaches based on fuzzy cognitive maps,” *Energies*, vol. 11, no. 3, 2018, doi: 10.3390/en11030495.
- [12] T. Ferhatbegovic, P. Palensky, G. Fontanella, and D. Basciotti, “Modelling and design of a linear predictive controller for a solar powered HVAC system,” *IEEE Int. Symp. Ind. Electron.*, pp. 869–874, 2012, doi: 10.1109/ISIE.2012.6237203.
- [13] I. S. Técnico, “IMPROVEMENT SUDOE INTERREG EU Project -DELIVERABLE D3.2.1. Report on Technical Specification of the IMPROVEMENT heating and cooling system.”
- [14] A. L. Nash, A. Badithela, and N. Jain, “Dynamic modeling of a sensible thermal energy storage tank with an immersed coil heat exchanger under three operation modes,” *Appl. Energy*, vol. 195, pp. 877–889, 2017, doi: 10.1016/j.apenergy.2017.03.092.
- [15] A. Rahman, N. Fumo, and A. D. Smith, “Simplified modeling of thermal storage tank for distributed energy heat recovery applications,” *ASME 2015 9th Int. Conf. Energy Sustain. ES 2015, collocated with ASME 2015 Power Conf. ASME 2015 13th Int. Conf. Fuel Cell Sci. Eng. Technol. ASME 2015 Nucl. Forum*, vol. 2, no. June, 2015.
- [16] E. e S. S. Ministérios do Ambiente, Ordenamento do Território e Energia e da Solidariedade, “Portaria n.º 349-D/2013 de 2 de dezembro dos Ministérios do Ambiente, Ordenamento do Território e Energia e da Solidariedade, Emprego e Segurança Social,” *Diário da República*, no. 40, p. 34, 2013.

Appendix

A_{coil}	Area of the coil heat exchanger in the tank	A_{loss}	Area of the tank in contact with the room	A_o	Area used for the losses in the fan coil
A_c	Area of the collector	A_{fc}	Area of the contact of the water and air in the fan coil	c_{p_a}/c_{p_w}	Air/water heat capacity
h	Heat transfer coefficient for losses in the fan coil	N_r	Number of rooms in contact with Room i	\dot{Q}_c	Useful heat in the solar collector
T_{cin}/T_{cout}	Inlet/Outflow temperature of solar collector	T_{tout}	Outflow temperature of the hot water tank	T_{ain}/T_{aout}	Inlet /Outflow temperature of the air in the fan coil
T_a	Ambient temperature	T_j	Temperature of the layer of the tank considered	T_{j-1}/T_{j+1}	Temperature of the layer above/below
T_{win}/T_{wout}	Inlet/ Outflow temperature of the water in the fan coil	T_i	Temperature of Room i	T_k	Temperature of the Room k, in contact with room i
U_{L1}, U_{L2}	Overall heat transfer coefficients for losses in the solar collector	U_{coil}	Overall heat transfer coefficient in the coil heat exchanger	U_{fc}	Overall heat transfer coefficient of the fan coil
U_{loss}	Overall heat transfer coefficient for the losses to the room	V_a/V_w	Volume of air/water in the fan coil	V_{tank}	Volume of the layer of the tank
V_i	Volume of Room i	\dot{V}_{vent}	Volumetric flowrate of ambient air for ventilation	\dot{V}_c	Solar system volumetric flowrate
\dot{V}_a/\dot{V}_w	Volumetric flowrate of air/water in the fan coil	\dot{V}_t	Hot water volumetric flowrate from the tank	\dot{V}_{HVAC}	Volumetric flowrate of air from the fan coil
Δx	Height of the layer	η_0	Zero loss efficiency	ρ_a/ρ_w	Air/Water density